MDPI

Article

Model Analysis and Experimental Study of Lower Limb Rehabilitation Training Device Based on Gravity Balance

Jianping Wang †, **Yanpeng Kan** †, **Taisheng Zhang, Zhen Zhang** * and **Manman Xu**

School of Mechanical Engineering, Anhui Polytechnic University, Wuhu 241000, China;
wangjianping@ahpu.edu.cn (J.W.); kanyanp1028@163.com (Y.K.); zts_mcsw@163.com (T.Z.);
xumanman@ahpu.edu.cn (M.X.)

* Correspondence: zhangzhen@ahpu.edu.cn
† These authors contributed equally to this work.

Abstract: More hemiplegia patients tend to use equipment for rehabilitation training due to the lack of physical therapists and the low effect of manual training. Nowadays, lower limb rehabilitation training devices for patients in grade 2 of the Medical Research Council (MRC-2) scale are still scarce and have some issues of poor autonomy and cannot relieve the muscle weakness of patients. To address these problems, a prototype based on gravity balance was designed with the combination of springs and linkages to enable patients to passively experience the rehabilitation training in the state of balancing the gravity of lower limbs. The motion of the mechanism was analyzed to obtain the functional relation between the motor rotation angle and the joints' angle. Based on the principle of constant potential energy, a gravity balance mathematical model of the device was established, analyzed, and simulated. Moreover, through the training experiment, the results show that when subjects in three different weights were trained under the rehabilitation device with and without gravity balance, the required torques of the motor and EMG signal strength of the knee and hip joints decreased by a degree of significance, which verified the effectiveness of the device's gravity balancing characteristics for MRC-2 patients.

Keywords: lower limb rehabilitation; gravity balance; kinematic analysis; structural design

1. Introduction

1.1. Motivation

Traffic accidents, strenuous exercise, stroke, tumor, trauma and other diseases can easily cause the dysfunction of innervated limb motions, and then lead to hemiplegia [1]. The aging of the population is becoming more and more serious nowadays. Stroke occurs more frequently in the middle-aged and elderly. Stroke patients will have different degrees of motion and cognitive and neurological disorders, while 55–75% of stroke patients suffer from hemiplegia [2]. Hemiplegic patients mainly have symptoms such as dyskinesia, language disorder and unconsciousness.

Hemiplegia can be divided into mild paralysis, incomplete paralysis and total paralysis. The MRC scale is the best known and most commonly used muscle strength grading system for manual muscle testing (MMT) worldwide. It measures the patient's muscle strength according to the patient's performance when they resist against gravity [3], and then resist again resistance, which is then divided into eight levels. The Medical Research Council grading scale is shown in Table 1 [4,5]. It is mainly based on the degree of movement of the patient's muscles and joints when patients are given an instruction to move their limbs [6]. Existing rehabilitation training devices mostly serve MRC-3 to MRC-5 patients who can resist the gravity of their own limbs. However, there are few rehabilitation devices for MRC-2 hemiplegic patients' lower limbs who can only drive the horizontal movement of their joints.

Table 1. MRC grading—MMT.

Level	Standard of Evaluate
Level 0	No measurable or perceptible muscle contraction.
Level 1	Slight muscle contraction, but cannot cause joint movement.
Level 2	Able to perform full range joint movement under weight reduction state.
Level 3	Able to perform full range of motion while resisting gravity, but cannot resist resistance.
Level 4−	Active movement against gravity and slight resistance.
Level 4	Active movement against gravity and moderate resistance.
Level 4+	Active movement against gravity and strong resistance.
Level 5	Normal power.

1.2. Related Works—Research on Rehabilitation Training Methods

Hemiplegia could be caused by many pathologies and there are many interventions for the rehabilitation of specific conditions. The timing of the initiation of rehabilitation treatment strongly affects rehabilitation outcomes. Patients with hemiplegia are treated by surgery and pharmacological treatments at the initial stage of treatment, while in the middle and late stages, they should be treated with auxiliary rehabilitation training combined with the corresponding equipment to prevent or reduce the symptoms of joint stiffness, joint degeneration and muscle atrophy around the joints of hemiplegic limbs [6]. Rehabilitation training performs targeted joint movement and effectively improves the muscle strength of patients' limbs. This could help the patients with limb paralysis recover their motion function and gradually recover their self-care ability. Compared with artificial therapists, rehabilitation equipment has the advantages of a good training effect, strong pertinence, and low cost [7]. Some researchers investigated and analyzed the walking recovery status of subacute hemiplegic patients six months after discharge from the hospital [8,9]. The results showed that targeted rehabilitation plans must be specified for the patients, otherwise, the effect of rehabilitation treatment would be affected due to complications and other factors. At the same time, it also showed the importance of early rehabilitation after hemiplegia. Some authors compared the gait rehabilitation training of subacute hemiplegic patients assisted by terminal effector robots and ground robots with traditional gait rehabilitation training, the experimental results of which showed that robot therapy is more conducive to the rehabilitation of patients and reduces the labor force of rehabilitation therapists [10,11]. The kinematics data of subacute stroke patients in the process of robot-assisted treatment were analyzed to evaluate the time and space for the improvement of patients' motor ability, and on this basis, designated a better rehabilitation program [12]. A trial followed up the use of physical therapy and robot-assisted therapy in subacute stroke subjects [13]. The results showed that use of robot-assisted therapy was more effective in reducing sports injury.

1.3. Related Works—Research on Gravity Balance Device

There are also some related studies on the lower limb rehabilitation training equipment based on gravity balance. Among them, passive rehabilitation training devices for the muscle weakness of patients have attracted the attention of many researchers. Traditional rehabilitation treatment uses the buoyancy of water, crutches, walking aids, suspension devices [14] and air bags [15] to assist walking, provide force and reduce the weight of lower limbs. In the literature, in order to meet the rehabilitation training requirements of paralyzed patients, the patient's lower limbs are regarded as a 2R structure [16], the human lower limb rehabilitation equipment mechanism was designed using the Stephenson six-bar

mechanism and the gravity balance of human lower limbs was realized by combining the zero initial length spring to reduce the load of lower limbs' gravity on the rehabilitation mechanism. The gravity balance characteristics were verified using the moment method and potential energy conservation method, respectively. Based on the spring parallelogram with static passive balance ability, the exoskeleton mechanism of the limbs and body for walking training was established [17], which was connected with the fixed support through two spring parallelograms. According to the weight and height of the subjects, select the appropriate spring stiffness coefficient and the installation position of the spring, and balance the gravity of the mechanism and part of the human body. Some authors proposed a new type of single degree of freedom gravity balancer [18], which was based on the static balance mechanism and spring adjustment mechanism of a standard spring (parallelogram, steel wire and slider system, and cam follower mechanism). The tension spring is connected to the static balance mechanism to balance the payload. Its installation point is controlled by two cables which are driven by the spring adjustment mechanism. When different payloads are applied, the spring adjustment mechanism will act to adjust the spring mounting point to the appropriate position, sense the change of payloads, and adjust the spring connection points accordingly to balance different payloads. A study proposed a passive method to compensate the torque on each joint [19], including a decoupling mechanism to isolate the torsional effect between various linkage mechanisms, and an achievable torsional compliant beam, which can provide a specific torsional stiffness function to compensate the torque due to the weight of the arm, and proposed an algorithm to reduce the joint torque required for gravity compensation. Two motors were installed at the hip joint and knee joint, and the torque sensors were used to detect the motor torque. In order to improve the force feedback perception accuracy of human opponents, some authors used the methods of adding counterweights and moving the hand grip point out of a certain distance from the wrist center, reduced the inertia force of the main hand, and achieved the gravity balance between the main hand and the wrist [20].

1.4. Contribution

Herein, we present a dynamic gravity-balance-based rehabilitation device for MRC-2 patients to address these aforementioned deficiencies. Patients in this level can do the full-range joint motion with the assistance of external devices to balance the most of lower limb gravity and overcome the rest of the gravity which is a small amount by themselves. Considering that the main motion joints of lower limbs are the hip and knee joint, which are also the main load-bearing joints, this study will focus on these two joints. The rehabilitation training device uses a combination of springs and auxiliary link rods to balance the gravity of the lower limb and the device, reducing the load on the muscles, enhancing the rehabilitation training effect, and abating the performance requirements of the driving equipment. The passive rehabilitation training of knee and hip joints for MRC-2 patients can be achieved in the sitting position and assist them during autonomous rehabilitation training, in order to gradually realize the initiative of patients' lower limbs, deepen muscle memory, avoid muscle atrophy, and regain walking ability.

2. Design of the Rehabilitation Device

The knee joint is the weight-bearing joint of the human body, which will be impacted when people do sport or improper exercise, and will easily cause damage to the meniscus and cruciate ligament. The human hip joint supports all the weight of the upper body which is heavily loaded. If the hip joint is unevenly loaded for a long time, it can lead to hip arthritis, femoral necrosis and joint pain, making it difficult to maintain standing and affecting hip joint movement.

2.1. Determine the Range of Joint Motion Angle

According to the simulation analysis of human gait [21] and playing football by opensim software [22–24], the knee joint and hip joint account for a large proportion of

flexion and extension activities in the sagittal plane. Therefore, the main research purpose of this study was to design a lower limb rehabilitation training device to assist MRC-2 patients in performing sagittal knee and hip flexion and extension training in sitting posture.

As shown in Figure 1, focusing on the MRC-2 patients in the sitting position, the flexion and extension training of the knee and hip joints were performed separately on the sagittal plane. Based on ergonomics [25], the range of joint motion during training with the device was determined, as shown in Table 2 [26].
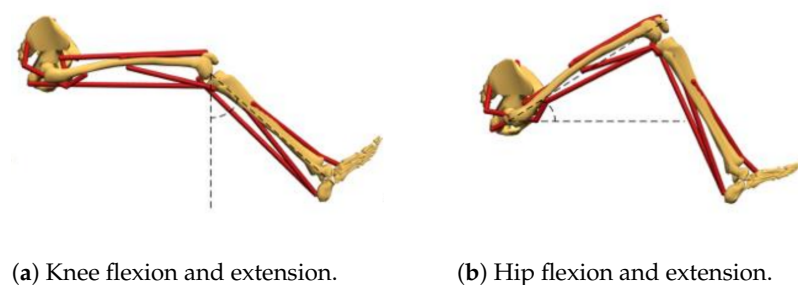

(**a**) Knee flexion and extension.　　　　　　　　(**b**) Hip flexion and extension.

Figure 1. Rehabilitation posture.

Table 2. Motion range of lower limb joints in sitting posture.

Category	Knee Joint Angle (°)	Hip Joint Angle (°)
Normal range of motion	0~30	0~30
Equipment's range	0~60	0~40

2.2. Design of Mechanism

The transmission mechanism consists of a crank linkage and a guide rod mechanism. The crank linkage mechanism and guide rod mechanism belong to the linkage transmission and move smoothly, whilst the transmission has a certain time difference, transmits the power from the motor to the training target, and avoids direct contact between the motor and the human body. If the motor encounters an accident such as power failure, it can also effectively prevent the patient getting injured and is suitable for rehabilitation training. Therefore, the crank linkage mechanism is selected to assist the knee flexion and extension training, and the guide rod mechanism assists hip flexion and extension training. The spring is set between the calf exoskeleton and the seat backrest, and the crank linkage mechanism and the spring work together to reduce the gravity of the calf and the device during knee flexion and extension training. Furthermore, set the spring between the thigh exoskeleton and the seat backrest, and the guide rod mechanism and spring work together to reduce the gravity of the lower limb and the device during hip flexion and extension training.

The three-dimensional model of the device is shown in Figure 2. The device is mostly composed of lower limb exoskeletons, springs, transmission mechanisms, moving mechanisms, and a drive system. To be suitable for different patients, the lower limb exoskeleton is designed to be adjustable in length for both the left and right lower limbs; the moving mechanism is composed of a cylinder and a push rod, which is fixed to the side of the chair; the transmission mechanism 1 and transmission mechanism 2 are for cranking the linkage mechanism and guiding the rod mechanism, respectively, which are driven by a motor to realize the rehabilitation training motion of the knee and hip joints; lower limb spring 1 is connected to the backrest and the lower end of the rod through a pulley and a traction device; and thigh spring 2 connects the front of the thigh pole with the backrest of the seat, and the position of the spring (the size of the elasticity changes with different installation positions) can be adjusted according to different people.
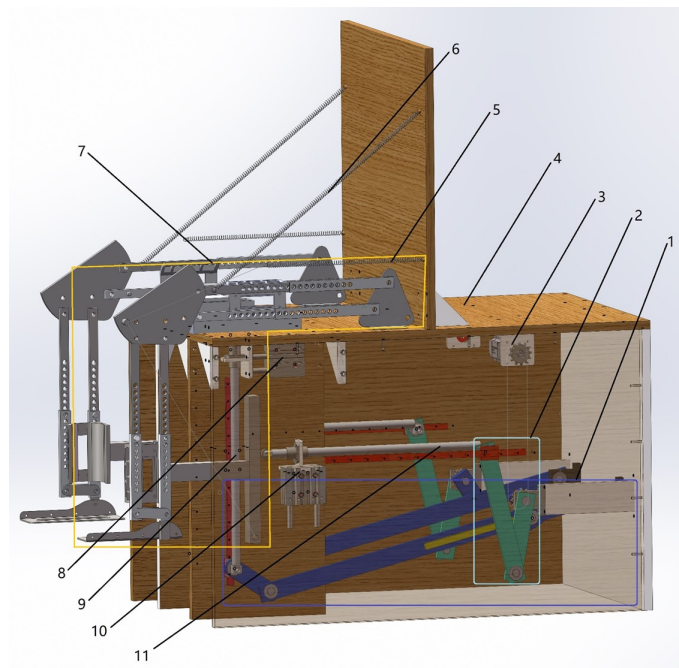
Figure 2. Three-dimensional diagram of the lower limb rehabilitation training device. 1—drive mechanism 2; 2—drive mechanism 1; 3—motor; 4—seat; 5—calf spring; 6—thigh spring; 7—lower limb exoskeleton; 8—cylinder 1; 9—thigh push rod; 10—cylinder 2; 11—calf push rod.

2.3. Principles of Rehabilitation Training

The rehabilitation training process of the knee joint is shown in Figure 3. Firstly, cylinder 2 drives the calf push rod to move upward, and when the calf pusher is in the same line as with the follower contacts of the crank linkage, cylinder 2 stops working. Then, the motor drives transmission mechanism 1 to work, and its follower comes into contact with the calf pusher to push the calf exoskeleton for knee rehabilitation. While the rehabilitation process is ongoing, calf spring 1 is working to compensate for the gravity of the knee joint during the process to achieve gravity balance. At the same time, transmission mechanism 2 also moves under the drive of the motor, but cylinder 1 does not work. Only the rehabilitation of the knee joint is carried out at this stage. When the calf returns to its vertical state, cylinder 2 drives the calf pusher to move down and one cycle of knee rehabilitation is completed.
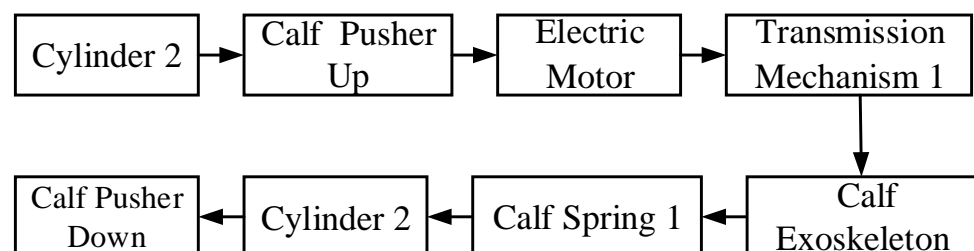

Figure 3. The rehabilitation training process of the knee joint.

The rehabilitation training process of the hip joint is shown in Figure 4. Firstly, cylinder 1 drives the thigh push rod to move to the right, and when the thigh push rod and the follower of transmission mechanism 2 are in the same straight line, cylinder 1 stops working. Then, the motor drives the transmission mechanism 2 to work, and its follower comes into contact with the thigh push rod to push the thigh exoskeleton for hip joint rehabilitation. At the same time, thigh spring 2 which connects the thigh exoskeleton and the seat backrest is used to compensate for the gravity of the hip joint during rehabilitation to achieve gravity

balance. The rotation angle of the motor is adjusted according to the patients' degree of injury to control the angle of the knee and hip joint flexion and extension to achieve the best rehabilitation effect.
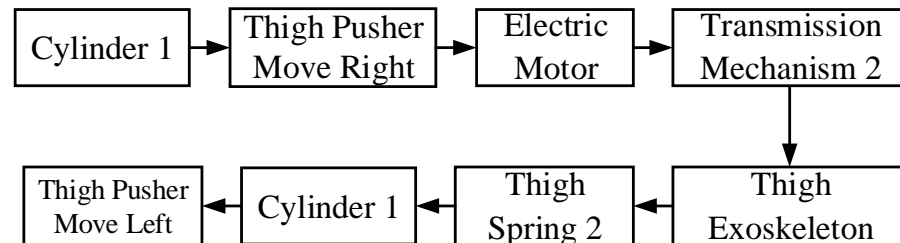

Figure 4. The rehabilitation training process of the hip joint.

3. Kinematic Analysis

According to the principle of rehabilitation training, the diagram of the hip joint rehabilitation training mechanism in sitting posture and its transmission mechanism motion variation diagram are shown in Figure 5. Furthermore, the diagrams of a knee joint are shown in Figure 6.
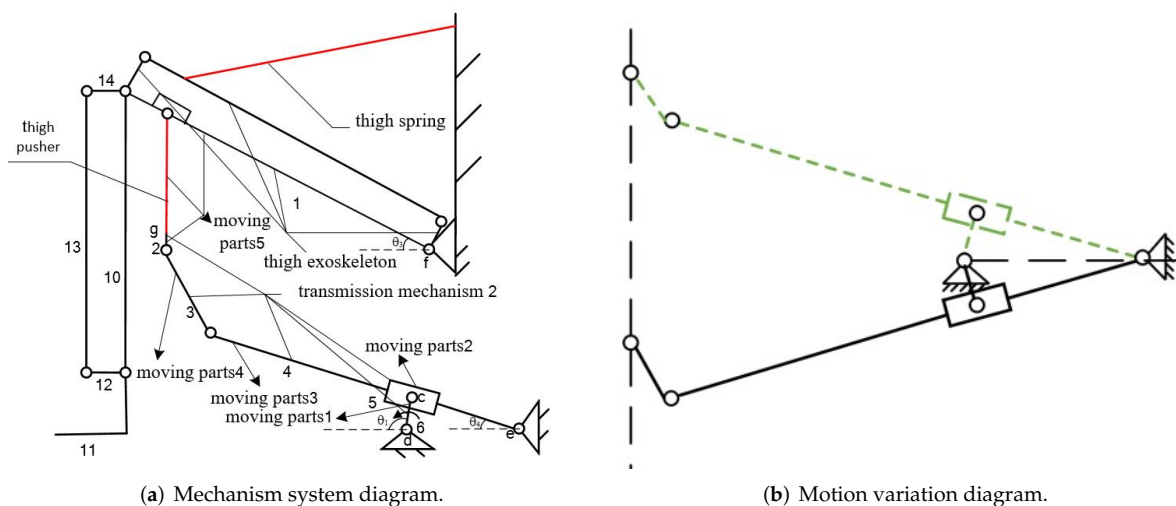

(**a**) Mechanism system diagram.　　(**b**) Motion variation diagram.

Figure 5. Hip joint rehabilitation transmission mechanism.

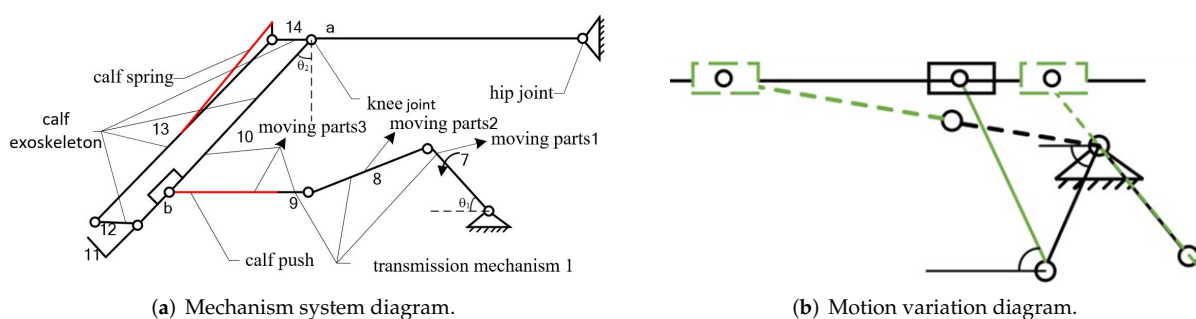(**a**) Mechanism system diagram.　　(**b**) Motion variation diagram.

Figure 6. Knee joint rehabilitation transmission mechanism.

There are four rotating and three movable pairs for knee rehabilitation. The hip joint has five movable pairs and seven rotating pairs during rehabilitation. According to the formula for calculating the degrees of freedom of the plane mechanism, we can obtain:

$$F_1 = 3n - 2P_L - P_H = 1 \tag{1}$$

$$F_2 = 3n - 2P_L - P_H = 1 \tag{2}$$

where F_1 is the degree of freedom of the knee rehabilitation mechanism, F_2 is the degree of freedom of the hip rehabilitation mechanism, n is the number of moving parts, P_L is the low pair and P_H is the high pair.

According to GB10000-1988—the standard body dimensions of Chinese adults [27]—the adjustable lengths of the thigh rod and calf rod were, respectively, determined to be 340~430 mm and 410~520 mm. According to the limit angle of joint training recorded in human physiology [28], the goal of rehabilitation and ensuring the safety of patients during rehabilitation training, the length of the transmission mechanism was determined and the specific parameters are shown in Table 3.

Table 3. Dimensions of the transmission mechanism.

Institution	Rods	Size (mm)
Transmission mechanism 1	Moving part 1	167
	Moving part 2	290
	Component 9	10
	Calf push rod	520
Transmission mechanism 2	Moving part 1	52
	Moving part 3	825
	Moving part 4	100
	Component 2	10
	Thigh push rod	520

The crank connecting rod is designed as a bias structure with a bias distance of 118 mm, and the horizontal distance of the guide rod mechanism is fixed at 885 mm. When the crank turns 360°, the crank linkage, the calf push rod, and the calf spring work together to complete a flexion or extension movement of the knee joint, and the relationship between the angle that the motor turns through and the angle of the calf extension is shown in Equation (3):

$$l_7 \cos\theta_1 + \sqrt{l_8^2 - (167 sin\theta_1 - 118)^2} = l_{ab} \tan\theta_2 \tag{3}$$

when moving part 1 has turned 360°, the guide rod mechanism and thigh push rod work together to accomplish 40° of flexion of the lower limb in the sagittal plane and return the thigh to horizontal. The relationship between the angle that the motor turns through and the angle of thigh flexion or extension is shown in Equation (4).

$$153 + 825 \sin\theta_4 + 100 \sin\left(\arccos\left(\frac{885 - 825 \cos\theta_4}{100}\right)\right) = l_{gf} \tan\theta_3 \tag{4}$$

The relationship between θ_4 and θ_1 is expressed as:

$$\theta_4 = \arctan\left(\frac{l_{cd} \sin\theta_1}{l_{de} + l_{cd} \cos\theta_1}\right) \tag{5}$$

where θ_4 is the rotation angle of moving part 3; and l_{gf} is the horizontal distance of the hip joint from the thigh push rod.

4. Analysis of Gravity Balance Characteristics

4.1. Establish the Model

Springs, auxiliary link rods and push rods were used to create an anti-gravity condition during the knee and hip joint rehabilitation training. The training models are shown in Figure 7. The motor is regarded as the frame and the coordinate established system while setting the motor as the coordinate origin. The mass of the rod is set as $m_1 \sim m_{16}$, the length of the rod is set as $L_1 \sim L_{19}$, the mass of the thigh is set as m_a, the length is set as L_a, the mass of the calf is set as m_b, the length is set as L_b, the mass of the foot is set as m_c and the length is set as L_c. In rehabilitation training, if the overall potential energy of the mechanism is always constant during the movement, then the system is in dynamic potential energy balance. Taking that as a premise, the springs' stiffness coefficient required for the system was calculated [29,30].
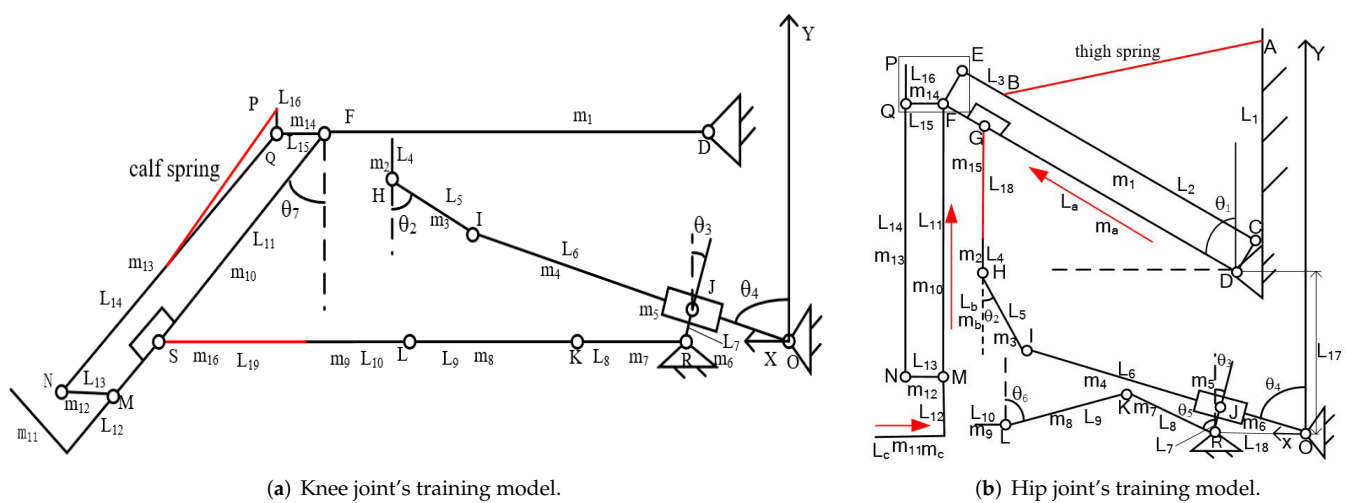

(**a**) Knee joint's training model.

(**b**) Hip joint's training model.

Figure 7. Rehabilitation training model of knee and hip joint.

To ensure the safety of the patient during rehabilitation training, according to the position of the transmission mechanism at the maximum potential energy, combined with the parameters in Table 3, the corresponding angle and length of the rods were obtained, as shown in Tables 4 and 5, respectively. The masses of the thigh, calf and foot were taken from the data of the obese type of human body and compared to standard weight, and the mass of each component was measured in an assembly drawing of SolidWorks, as shown in Table 6.

Table 4. Angles of the rods at the position of maximum potential energy.

Angle	θ_1	θ_2	θ_3	θ_4	θ_5	θ_6	θ_7
Value (°)	40	53	36	77	0	45	60

Table 5. Length of each rod.

Rods	L_1	L_2	L_3	L_4	L_5	L_6	L_7	L_8	L_9	L_{10}	L_{11}
Length (mm)	506	419	40	10	100	825	52	167	290	10	370
Rods	L_{12}	L_{13}	L_{14}	L_{15}	L_{16}	L_{17}	L_{18}	L_{19}	L_a	L_b	L_c
Length(mm)	60	70	370	70	44	458	213	520	270	270	10

Table 6. Mass of each component and lower limbs.

Parts	m_1	m_2	m_3	m_4	m_5	m_6	m_7	m_8	m_9	m_{10}
Mass (kg)	0.256	0.023	0.044	0.118	0.011	0.039	0.078	0.041	0.023	0.089
Parts	m_{11}	m_{12}	m_{13}	m_{14}	m_{15}	m_{16}	m_a	m_b	m_c	
Mass (kg)	0.577	0.009	0.089	0.239	0.426	0.426	8.3	4.5	1.2	

4.2. Potential Energy Analysis of Knee Joint Rehabilitation Training System

The gravity balance model for knee rehabilitation training is shown in Figure 5, during calf flexion and extension training, wherein the thigh push rod does not work and transmission mechanism 2 performs a no-load motion because the device uses a single motor to drive 2 degrees of freedom. Therefore, the potential energy of each part needs to be calculated separately. Calculation formula of the gravitational potential energy W_1 of transmission mechanism 2:

$$W_1 = m_2(\frac{L_4}{2} + L_5 \cos\theta_2 + L_6 \cos\theta_4)g + m_3(\frac{L_5}{2}\cos\theta_2 + L_6 \cos\theta_4)g + m_4(\frac{L_5}{2}\cos\theta_4)g$$
$$+ m_5(L_7 \cos\theta_3)g + m_6(\frac{L_7}{2}\cos\theta_3)g \tag{6}$$

Substituting the values of each parameter into Equation (6) can obtain:

$$W_1 = 0.989 \text{ J}$$

Calculation formula of the gravitational potential energy W_2 of transmission mechanism 1 and calf pushers:

$$W_2 = (m_7 + m_8 + m_9 + m_{16})gh + m_7 g(\frac{L_8}{2}\cos\theta_5) + m_8 g(\frac{L_9}{2}\cos\theta_6) \tag{7}$$

Rods 7, 8, 9 and 16 are colinear with the x axis, where h = 0, and substituting the values of each parameter into Equation (7) can obtain:

$$W_2 = 0.23 \text{ J}$$

Calculation formula of the gravitational potential energy W_3 of the lower limb exoskeleton:

$$W_3 = (m_{10} + m_{11} + m_{12} + m_{13} + m_{14})g\, L_{17} - (m_{10} + m_{11})\, g\frac{L_{11} + L_{12}}{2}\cos\theta_7$$
$$- m_{13}\, g\frac{L_{14}}{2}\cos\theta_7 - m_{12}\, gL_{11}\cos\theta_7 \tag{8}$$

Calculation formula of the calf's gravitational potential energy W_4:

$$W_4 = (m_a + m_b + m_c)gL_{17} - m_b\, gL_b \cos\theta_7 - m_c\, g(L_c + L_{11} + L_{12})\cos\theta_7 \tag{9}$$

Calculation formula of elastic potential energy W_5 of calf spring 1:

$$W_5 = \frac{1}{2}k_1(\frac{L_{14}^2}{2} + L_{16}^2) + k_1\frac{L_{14}L_{16}}{2}\cos(180 - \theta_7) \tag{10}$$

when transmission mechanism 2 moves without load, its maximum potential energy is 0.98 J and the maximum potential energy of transmission mechanism 1 during the rehabilitation movement is 0.23 J. If the rehabilitation device can maintain equilibrium

in the case of maximum potential energy, the device can also maintain equilibrium in other states.

Calculation formula of spring stiffness coefficient when the gravity is balanced:

$$k_1 = \frac{(m_{10} + m_{11})g(L_{11} + L_{12}) + 2m_{12}\,gL_{11} + 2m_c\,g(L_c + L_{11} + L_{12}) + 2m_b\,gL_b + m_{13}gL_{14}}{L_{14}L_{16}} \tag{11}$$

Substituting the values of each parameter can obtain:

$$k_1 = 2.467 \; N/mm$$

4.3. Potential Energy Analysis of Hip Joint Rehabilitation Training System

The diagram of gravity balance for hip joint rehabilitation training is shown in Figure 6. During hip flexion and extension training, the calf push rod does not work and transmission mechanism 1 performs a no-load motion. Therefore, the potential energy of each part needs to be calculated separately. Calculation formula of the gravitational potential energy of transmission mechanism 2 and thigh push rod:

$$W_6 = (m_2 + m_{15})\left(\frac{L_{14} + L_{18}}{2} + L_5 \cos\theta_2 + L_6 \cos\theta_4\right)g + m_3\,g\left(\frac{L_5}{2}\cos\theta_2 + L_6 \cos\theta_4\right)$$
$$+ m_4\,g\frac{L_6}{2}\cos\theta_4 + m_5\,gL_7 \cos\theta_3 + m_6\,g\frac{L_7}{2}\cos\theta_3 \tag{12}$$

Substituting the values of the parameters into Equation (12) can obtain

$$W_6 = 16.3 \; J$$

Calculation formula of the gravitational potential energy W_7 of transmission mechanism 1:

$$W_7 = (m_7 + m_8 + m_9)gh + m_7\,g\frac{L_8}{2}\sin\theta_5 + m_8\,g\frac{L_9}{2}\sin\theta_6 \tag{13}$$

Rods 7, 8 and 9 are colinear with the x axis, and where h = 0, substitute the values of each parameter into Equation (13) to obtain:

$$W_7 = 0.2 \; J$$

Calculation formula of the gravitational potential energy of the lower limb exoskeleton W_8:

$$W_8 = (m_1 + m_{10} + m_{11} + m_{12} + m_{13} + m_{14})gL_{17} + \frac{L_{11} + L_{12}}{2}(m_{10} + m_{11})g$$
$$- m_{13}\,g\frac{L_{14}}{2} - -\cos\theta_1 \begin{pmatrix} m_{12}\,g(L_2 + L_3 + \frac{L_{13}}{2}) + \\ m_{13}\,g(L_2 + L_3 + L_{15}) + \\ (m_{10} + m_{11})(L_2 + L_3)g + \\ (m_1 + m_{14})\frac{L_2 + L_3 + L_{15}}{2}g \end{pmatrix} \tag{14}$$

Calculation formula of the gravitational potential energy of the calf and thigh W_9

$$W_9 = (m_a + m_b + m_c)gL_{17} - m_a gL_{17}\cos\theta_1 - m_b g[L_b + (L_2 + L_3)\cos\theta_1]$$
$$- m_c g[L_{11} + L_{12} + L_c + (L_2 + L_3)\cos\theta_1] \tag{15}$$

Calculation formula of elastic potential energy W_{10} of thigh spring 2:

$$W_{10} = k_2\left(\frac{L_1^2 + L_2^2}{2} - L_1 L_2 \cos\theta_1\right) \tag{16}$$

The maximum potential energy of drive mechanism 2 during the hip joint rehabilitation training is 16.3 J. The maximum potential energy of drive mechanism 1 during the no-load movement is 0.2 J. If the rehabilitation device can maintain equilibrium in the case of maximum potential energy, the device also maintains equilibrium in other states.

The calculation formula of the spring stiffness coefficient when the gravity is balanced:

$$k_2 = \frac{1}{L_1 L_2}\left(\begin{array}{l} m_{12}g(L_2 + L_3 + \frac{L_{13}}{2}) + (m_1 + m_{14})g\frac{L_2 + L_3 + L_{15}}{2} + \\ (m_{10} + m_{11})g(L_2 + L_3) + m_{13}g(L_2 + L_3 + L_{15}) + \\ m_a g L_a + m_b g(L_2 + L_3) + m_c g(L_2 + L_3) \end{array}\right) \quad (17)$$

Substituting the values of the parameters into Equation (17) can obtain:

$$k_2 = 0.247 \; N/mm$$

where k_2 is the required spring stiffness coefficients, respectively, in the state when the knee and hip joint rehabilitation training mechanism is at maximum potential energy, then set it into the simulation software.

4.4. Simulation Analysis of the Rehabilitation Training Device Model

The virtual prototype model of the lower limb rehabilitation training device was built in ADAMS software according to the model parameters. Based on the standard human body weight, patients of three body types, namely lean, normal and obese, were selected to conduct the simulation test of the knee and hip joint rehabilitation training in ADAMS software with and without gravity balance in two cases (as shown in Figure 8). The weights of their lower limbs and thighs are shown in Table 7.

Table 7. Lower limb weights of patients with different body types.

Limb Parts (kg)	Thin	Normal	Obese
Calf	3	3.7	4.5
Thigh	5.1	6.4	8.3

(**a**) Knee flexion and extension.　　　(**b**) Hip flexion and extension.
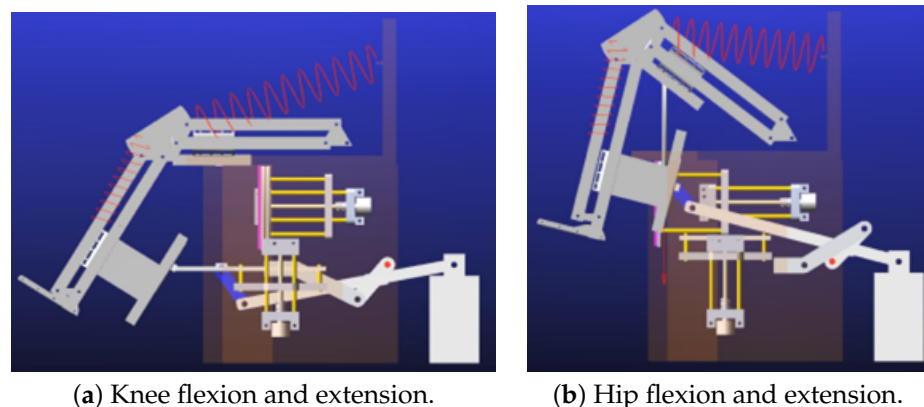
Figure 8. Knee and hip joint simulation process.

The human lower limb mass was matched to the center of mass of the exoskeleton, the simulation time was set to 60 s, and the number of simulation steps was 2000. The motor torque variations of the three body types' patients during the simulation test of the knee joint flexion and extension training with and without gravity balance were measured as shown in Figure 9, and the simulation test of hip joint is also shown in Figure 10.
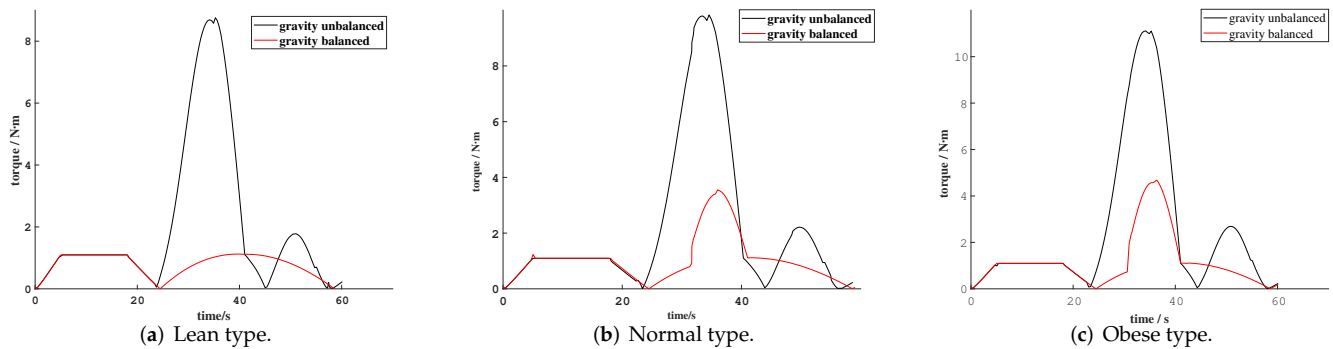
(a) Lean type. **(b)** Normal type. **(c)** Obese type.

Figure 9. Motor torque variations during knee rehabilitation training with 3 different weights.

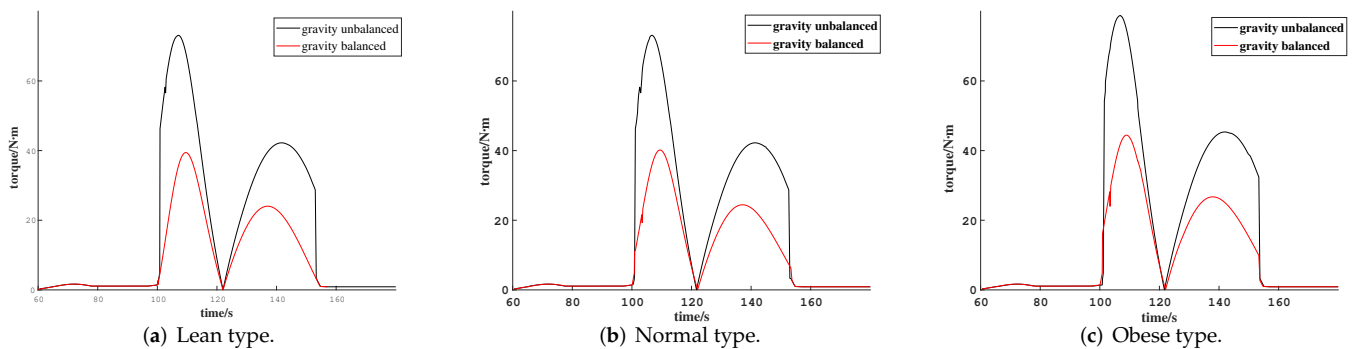**(a)** Lean type. **(b)** Normal type. **(c)** Obese type.

Figure 10. Motor torque variations during hip rehabilitation training with 3 different weights.

From Figure 9, it is distinct that during the knee joint rehabilitation training, the first 0–25 s is the drive mechanism 1 for the no-load motion. After 25 s, the exoskeleton device drives the calf for motion, and the torque will suddenly increase at the moment that the calf is lifted. During the training process, the calf's gravity is balanced by spring 1 and the auxiliary link rod. A reciprocating calf kicking training motion is completed within 25–60 s. Due to the existence of the linkage's gravity, the curve of the torque presents a parabola with the opening downward. The motor torque of three different types of patients all showed a significant decrease compared to when they trained with and without gravity balance during the knee joint rehabilitate training, and their specific torque values are compared as shown in Table 8. This demonstrates that the device can achieve gravity balance while the knee joint is doing the rehabilitation action, which verifies the rationality of the mechanism and the parameters were set correctly, thus it can be applied to the knee joint rehabilitation training for MRC-2 patients.

Table 8. Comparison of maximum moments during knee rehabilitation.

Status of Rehabilitation Equipment	Maximum Torque of Lean Type (N·m)	Maximum Torque of Normal Type (N·m)	Maximum Torque for Obese Type (N·m)
Gravity balanced	1.12	3.5	4.7
Gravity unbalanced	8.8	9.8	11.1

From Figure 10, it can be seen that during the hip rehabilitation training process, in 60–100 s, it is the transmission mechanism that carries out the no-load motion. After 100 s, the exoskeleton drives the thigh to carry out the lower limb lifting motion, and when the

thigh is lifted, the torque will suddenly increase. Furthermore, the gravity of the thigh and calf is balanced by spring 2 and the transmission mechanism. A reciprocal thigh lifting training motion is completed in 100–122 s. The curve of the torque presents a parabola with downward opening. The result of Figure 10 is very similar to that of Figure 9. The gravity of the hip joint of three types of patients is also effectively offset in rehabilitation training, which again verifies the rationality of the device. Specific torque values are compared as shown in Table 9.

Table 9. Comparison of maximum torque during hip rehabilitation.

Status of Rehabilitation Equipment	Maximum Torque of Lean Type (N·m)	Maximum Torque of Normal Type (N·m)	Maximum Torque for Obese Type (N·m)
Gravity balanced	39.0	40.1	44.4
Gravity unbalanced	68.8	73.1	78.7

From Tables 8 and 9, it can be seen that the motor torque required for the rehabilitation training of the knee joint was reduced, respectively, by 87.3%, 64.3% and 57.7%, and for the hip joint rehabilitation training, it was reduced by 43.3%, 45.1% and 43.6%. According to the results, the device can reduce the muscle force and the energy consumption of the system, which can verify that the device can effectively achieve gravity balance.

5. Experiment

To verify the simulation results, a test prototype of the lower limb rehabilitation training device was developed, with the power transmission system using an electric motor as the drive unit, a touch controller as the core of the control system, and a crank link rod and guide rod mechanism as the transmission mechanism, as shown in Figure 11. Table 10 shows the parameter table of the prototype machine, and the whole device is made of aluminum alloy. As the controller selects rehabilitation mode to control the servo motor and realize the rehabilitation training, the control process is shown in Figure 12.
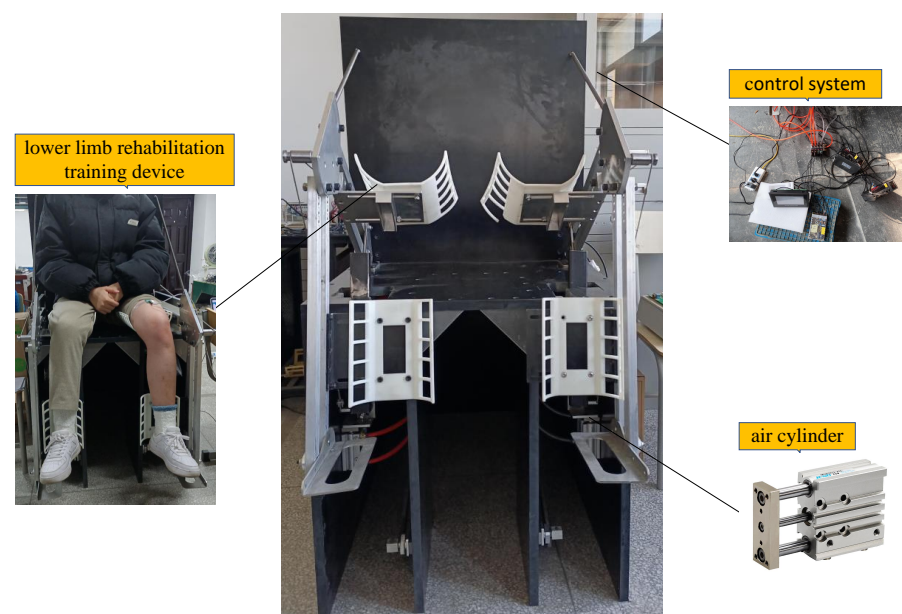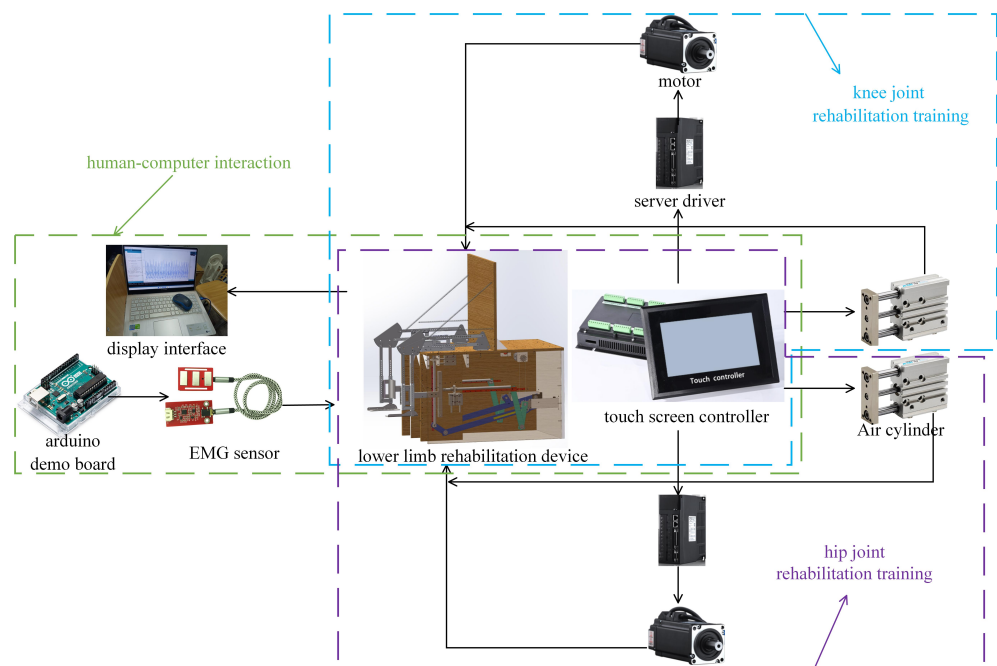

Figure 11. Lower limb rehabilitation training device prototype.

Table 10. Component selection of prototype.

Parameters	Numerical Value
Materials	Aluminum alloy 6061
Drive motor	MODEL SUPSM-T-H2-130-15015-AP1B61
Cylinder	J-MGPM20 × 50Z
Touch screen controller	QL7B-2 Dual Axis

Figure 12. Schematic diagram of the control process.

Three subjects with large differences in body size were selected, and their heights and weights are shown in Table 11. The prototype for rehabilitation training tests was used to verify whether the training device can fulfill the training movement and gravity balance characteristics of the device. The rehabilitation training posture is shown in Figure 13.

Table 11. Comparison of maximum torque during hip rehabilitation.

Subjects	Height (cm)	Age	Body Weight (kg)
1	166	20	53
2	172	25	70
3	181	23	86

The degree of contraction represents the amount of muscle strength generated during the rehabilitation training. Since the rectus femoris muscle is directly involved in the knee and hip joint flexion and extension, we placed an EMG sensor close to the rectus femoris muscle area of the experimenter, as shown in Figure 13a, to collect the muscles' surface EMG signals for knee and hip flexion and extension separately [31–33].
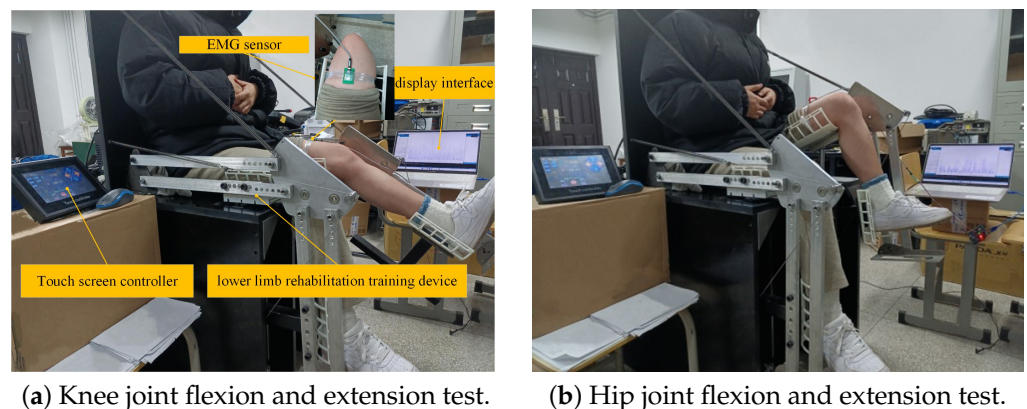
(**a**) Knee joint flexion and extension test.　　(**b**) Hip joint flexion and extension test.

Figure 13. Schematic diagram of the control process.

Randomly select 100 signals from the 1000 samples of a flexion and extension cycle collected by the EMG sensor, and fit the curve with MATLAB. The changes of surface EMG signals of rectus femoris in three cases were compared in three different situations: the subjects' lower limbs were in a calm state, the subjects performed knee and hip joint flexion and extension autonomously, and the subjects were assisted with the gravity balance lower limb rehabilitation training device.

6. Discussion

In the above experiment, we tested three subjects in three states during the knee and hip joint rehabilitation training, respectively, as shown in Figure 14. It can be seen that the EMG signal strength of rectus femoris during rehabilitation with the gravitational balance lower extremity rehabilitation device remained almost unchanged compared to the calm time, while the EMG signal strength decreased compared to the knee and hip joint flexion and autonomously performed extension exercises, as shown in Table 12. The average decrease in EMG signal strength for the three subjects was 87% for knee joint rehabilitation and 81% for hip joint rehabilitation.

Table 12. Percentage decrease in EMG signals' intensity during joint rehabilitation.

Subjects	During Knee Joint Rehabilitation	During Hip Joint Rehabilitation
Subject 1	97%	75%
Subject 2	93%	84%
Subject 3	71%	83%

In conclusion, our results showed that most of the gravity of the subjects' lower limbs is offset by the device. The lower limb muscles of the subjects only need to force a little in the process of rehabilitation training, which indicates that it could enable MRC-2 patients to actively complete the whole range of the joint movement. The results verified that the device can achieve dynamic balance in the whole training process and solve the problem that only static gravity balance can be achieved, highlighted in references [17,20].

Additionally, at the end of rehabilitation training, the EMG signal curve is still in stable attenuation, and there is no inertial impact situation. At the beginning of the design, the range of motion of the patient's lower limbs is taken into account, and the transmission device is specifically designed so that the safety of the patient is also guaranteed. This also avoids problems of inertial impact and insufficient safety when using the counterweight method to balance the limb gravity in references [19,20].
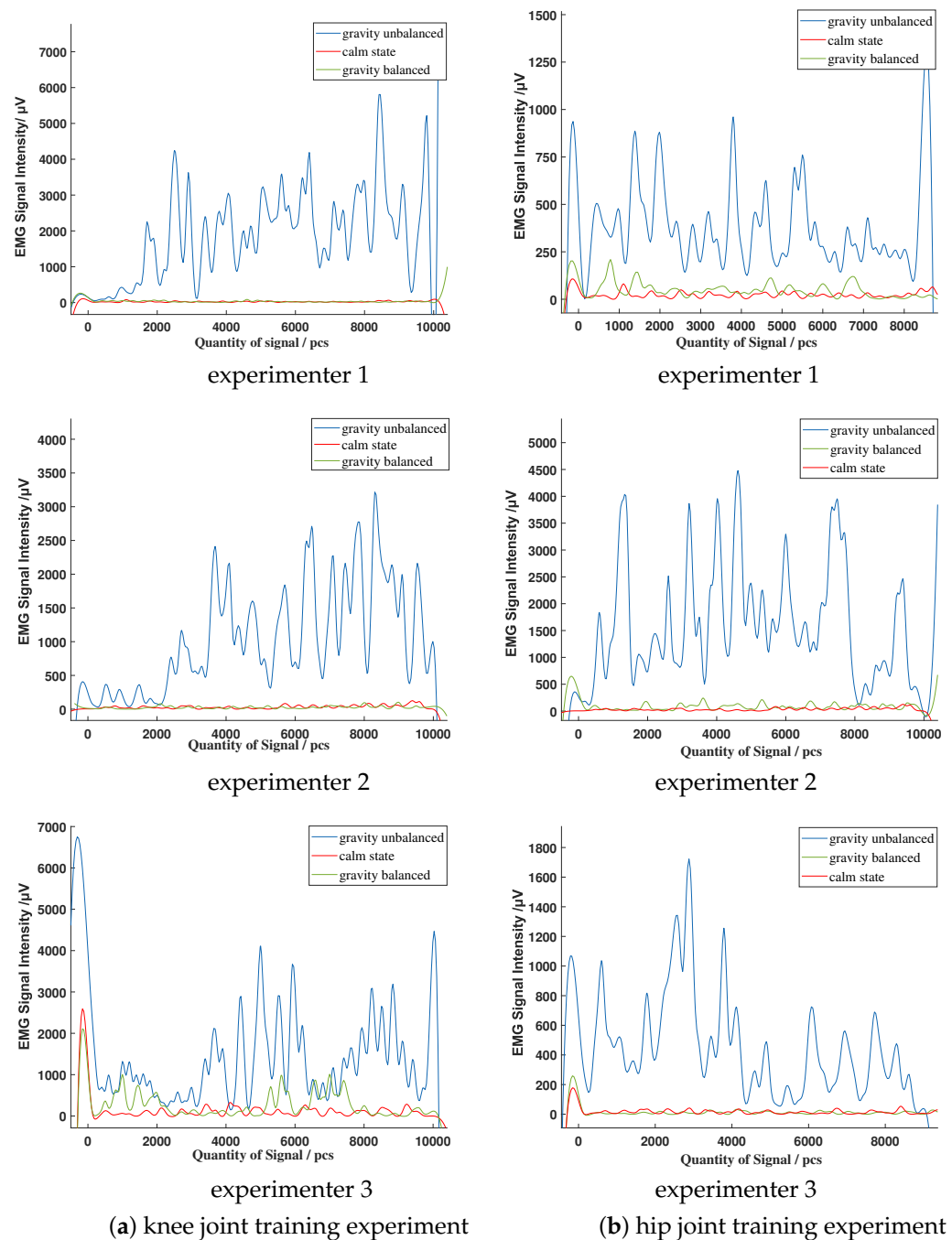
(**a**) knee joint training experiment (**b**) hip joint training experiment

Figure 14. EMG signal variation of subjects during rehabilitation training experiment.

Compared with the method of controlling the compensation torque in reference [19], the device designed in this paper does not need to install a motor at the lower limbs' joints, which improves the problems of high performance requirements for the driving equipment and high-energy consumption of the system and avoids the unstable inertia impact at the end of rehabilitation.

In future works, we will consider enhancing the control of the motor and accelerating the response speed of the device. At the same time, we noticed noise which was generated during the operation of the device which needs to be reduced.

7. Conclusions

(1) In this paper, the shortcomings of existing gravity balance devices were considered synthetically and then, based on the ergonomic and bionic perspectives, a new gravity balanced lower limb rehabilitation training device was designed. This can assist MRC-2 patients in performing knee and hip joint flexion and extension training in the motion range of human motion in a sitting position.

(2) The kinematic analysis of the mechanism was conducted to obtain the relationship between the motor rotation angle and joints' flexion and extension angle. A mathematical model of knee and hip joint training based on gravity balance was established to analyze the gravity balance characteristics of the system. Furthermore, the required spring stiffness coefficient was calculated.

(3) A virtual prototype of the lower limb rehabilitation training device was established and the lower limb mass of the subjects with three different types of body sizes was set at the centroid of the exoskeleton. The knee and hip joint flexion and extension simulation tests were conducted to verify the gravity balance characteristics of the device and the rationality of the device by comparing the motor torque in cases with and without gravity balance.

(4) The physical prototype and the control platform were produced, and three subjects with huge differences in body size were selected to perform knee and hip joint flexion and extension training tests. Based on the strength of the EMG signal to verify the feasibility of the gravity balancing scheme, the gravity of the lower limbs and the device is balanced according to the test results. The device reduced the need for muscle strength, enhanced the effect of rehabilitation training, and reduced the requirements for the performance of the drive equipment.

References

1. Zhang, J.; Mu, Y.; Zhang, Y. Effects of Acupuncture and Rehabilitation Training on Limb Movement and Living Ability of Patients with Hemiplegia after Stroke. *Behav. Neurol.* **2022**, *2022*, 2032093. [CrossRef] [PubMed]
2. Hwang, S.; Lee, S.; Shin, D.; Baek, I.; Ham, S.; Kim, W. Development of a Prototype Overground Pelvic Obliquity Support Robot for Rehabilitation of Hemiplegia Gait. *Sensors* **2022**, *22*, 2462. [CrossRef]
3. Saranya, S.; Poonguzhali, S.; Karunakaran, S. Gaussian mixture model based clustering of Manual muscle testing grades using surface Electromyogram signals. *Phys. Eng. Sci. Med.* **2020**, *43*, 837–847. [CrossRef] [PubMed]
4. Gregson, J.M.; Leathley, M.J.; Moore, A.P.; Smith, T.L.; Sharma, A.K.; Watkins, C.L. Reliability of measurements of muscle tone and muscle power in stroke patients. *Age Ageing* **2000**, *29*, 223–228. [CrossRef]
5. Paternostro-Sluga, T.; Grim-Stieger, M.; Posch, M.; Schuhfried, O.; Vacariu, G.; Mittermaiier, C.; Bittner, C.; Fialka-Moser, V. Reliability and validity of the Medical Research Council (MRC) scale and a modified scale for testing muscle strength in patients with radial palsy. *J. Rehabil. Med.* **2008**, *40*, 665. [CrossRef]

6.   Virani, S.S.; Alonso, A.; Aparicio, H.J.; Benjamin, E.J.; Bittencourt, M.S.; Callaway, C.W.; Carson, A.P.; Chamberlain, A.M.; Cheng, S.; Delling, F.N.; et al. Heart Disease and Stroke Statistics—2021 Update: A Report From the American Heart Association. *Circulation* **2021**, *143*, 254–743. [CrossRef]
7.   Ullas, U.; Rajendrakumar, P.K. Design of a Low-Cost Lower Limb Rehabilitation Exoskeleton System. *IOP Conf. Ser. Mater. Sci. Eng.* **2021**, *1132*, 012008. [CrossRef]
8.   Pournajaf, S.; Goffredo, M.; Agosti, M.; Massucci, M.; Ferro, S.; Franceschini, M.; Italian Study Group on Implementation of Stroke Care (ISC Study). Community ambulation of stroke survivors at 6 months follow-up: An observational study on sociodemographic and sub-acute clinical indicators. *Eur. J. Phys. Rehabil. Med.* **2019**, *55*, 433–441. [CrossRef]
9.   Carlo, A.D.; Lamassa, M.; Franceschini, M.; Bovis, F.; Cecconi, L.; Pournajaf, S.; Paravati, S.; Biggeri, A.; Inzitari, D.; Ferro, S.; et al. Impact of acute-phase complications and interventions on 6-month survival after stroke. A prospective observational study. *PLoS ONE* **2018**, *13*, e0194786. [CrossRef]
10.   Aprilea, I.; Iacovelli, C.; Goffredo, M.; Cruciani, A.; Franceschini, M. Efficacy of end-effector Robot-Assisted Gait Training in subacute stroke patients: Clinical and gait outcomes from a pilot bi-centre study. *NeuroRehabilitation* **2019**, *45*, 1–12. [CrossRef]
11.   Molteni, F.; Guanziroli, E.; Goffredo, M.; Calabrò, R.; Franceschini, M. Gait Recovery with an Overground Powered Exoskeleton: A Randomized Controlled Trial on Subacute Stroke Subjects. *Brain Sci.* **2021**, *11*, 104. [CrossRef]
12.   Goffredo, M.; Mazzoleni, S.; Gison, A.; Infarinato, F.; Pournajaf, S.; Galafate, D.; Agosti, M.; Posteraro, F.; Franceschini, M. Kinematic parameters for tracking patient progress during upper limb robot-assisted rehabilitation: An observational study on subacute stroke subjects. *Appl. Bionics Biomech.* **2019**, *2019*, 4251089 . [CrossRef]
13.   Franceschini, M.; Mazzoleni, S.; Goffredo, M.; Pournajaf, S.; Galafate, D.; Criscuolo, S.; Agosti, M.; Posteraro, F. Upper limb robot-assisted rehabilitation versus physical therapy on subacute stroke patients: A follow-up study. *J. Bodyw. Mov. Ther.* **2020**, *24*, 194–198. [CrossRef]
14.   Reed, J.A. Research progress in weight reduction training. *Chin. J. Phys. Med. Rehabil.* **2002**, *24*, 58–60.
15.   Zhao, J.; Zou, R.; Xu, X.; Hu, X. Design and Analysis of Body Weight Support Based Treadmill for Lower Limb Rehabilitation Training. *Prog. Biomed. Eng.* **2014**, *35*, 187–190.
16.   Jing, M.K. A dissertation submitted in partial fulfillment of the requirements for the academic degree of Master of Engineering. Master's Thesis, Harbin Institute of Technology, Harbin, China, 2019.
17.   Chen, Z.P. Conceptual Study of a Passive Exoskeleton System for Reduced Gravity Locomotion Training for Astronaut. Master's Thesis, Nanjing University of Aeronautics & Astronautics, Nanjing, China, 2014.
18.   Chu, Y.L.; Kuo, C.H. A Single-DoF Self-Regulated Gravity Balancer for Adjustable Payload. *J. Mech. Robot.* **2017**, *9*, 1–8. [CrossRef]
19.   Cheng, Z.; Foong, S.; Sun, D.; Tan, U.X. Towards a multi-DOF passive balancing mechanism for upper limbs. In Proceedingd of the International Conference on Rehabilitation Robotics, Singapore, 11–14 August 2015; pp. 508–513. [CrossRef]
20.   Xu, W.; Chen, Z.; Fan, R.; Wen, X. Improve the Wrist Structure of the Haptic Master under Gravity Balance. *Mech. Sci. Technol. Aerosp. Eng.* **2017**, *36*, 196–201.
21.   Mei, Q.; Gu, Y.; Dong, S.; Li, J.; Fernandez, J. Review on the Application of Image-Based Subject-Specific OpenSim Lower Extremity Musculoskeletal Model into Biomechanics Research. *J. Med. Biomech.* **2019**, *35*, 259–264.
22.   Zhou, M.; Huang, Q.; Jiang, X. Progress in the application of gait analysis in orthopedic and physical rehabilitation. *J. Orthop. Clin. Res.* **2021**, *6*, 243–249.
23.   Xie, E.; Zhan, J. Progress in big data analysis of gait biomechanics. *J. Med. Biomech.* **2021**, *36*, 984–989.
24.   You, Y.; He, W.H.; Song, Q.Y. Progress in the application of different gait analysis systems in osteoarthritis. *Sci. Technol. Her.* **2021**, *39*, 35–42.
25.   Yulan, D. *Ergonomics*, 4 ed.; Beijing Institute of Technology Press: Beijing, China, 2011.
26.   Chao, H.; Yun, G.; Ying., C. Human joint mobility measurement system. *Chin. J. Med. Phys.* **2016**, *33*, 34–38.
27.   *GB 10000-88*; Human Dimensions of Chinese Adults. China Association for Standardization: Beijing, China, 1988.
28.   Karl, H.E.; Kroemer, H.J.; Kroemer, K.E. *Engineering Physiology*, 4 ed.; Springer: Berlin/Heidelberg, Germany, 2010.
29.   Gianluca, G.; Giuseppe, C. Gravity Compensation of Robotic Manipulators Using Non-linear Spring Configurations. In Proceedings of the International Conference of IFToMM ITALY, Online, 9–11 September 2020; pp. 310–317. [CrossRef]
30.   Tschiersky, M.; Hekman, E.; Brouwer, D.M.; Herder, J.L. Gravity Balancing Flexure Springs for an Assistive Elbow Orthosis. *IEEE Trans. Med. Robot. Bionics* **2019**, *1*, 177–188. [CrossRef]
31.   Shi, X.; Qin, P.; Zhu, J.; Zhai, M.; Shi, W. Feature Extraction and Classification of Lower Limb Motion Based on sEMG Signals. *IEEE Access* **2020**, *8*, 132882–132892. [CrossRef]
32.   Khoshdel, V.; Akbarzadeh, A.; Naghavi, N.; Sharifnezhad, A.; Souzanchi-Kashani, M. sEMG-based impedance control for lower-limb rehabilitation robot. *Intell. Serv. Robot.* **2018**, *11*, 97–108. [CrossRef]
33.   Petersen, I.L.; Nowakowska, W.; Ulrich, C.; Struijk, L.N.S.A. A Novel sEMG Triggered FES-Hybrid Robotic Lower Limb Rehabilitation System for Stroke Patients. *IEEE Trans. Med Robot. Bionics* **2020**, *2*, 631–638. [CrossRef]